



Contribution to the Symposium: 'Marine Acoustics Symposium'

Original Article

Deep-scattering layer, gas-bladder density, and size estimates using a two-frequency acoustic and optical probe

Rudy J. Kloster*, Tim E. Ryan, Gordon Keith, and Lisa Gershwin

CSIRO Oceans and Atmosphere Flagship, PO Box 1538, Hobart, TAS 7001, Australia

*Corresponding author: e-mail: rudy.kloster@csiro.au

Kloster, R. J., Ryan, T. E., Keith, G., and Gershwin, L. Deep-scattering layer, gas-bladder density, and size estimates using a two-frequency acoustic and optical probe. – ICES Journal of Marine Science, 73: 2037–2048.

Received 28 August 2015; revised 25 November 2015; accepted 2 December 2015; advance access publication 26 January 2016.

Estimating the biomass of gas-bladdered organisms in the mesopelagic ocean is a simple first step to understanding ecosystem structure. An existing two-frequency (38 and 120 kHz) acoustic and optical probe was lowered to 950 m to estimate the number and size of gas-bladders. *In situ* target strengths from 38 and 120 kHz and their difference were compared with those of a gas-bladder resonance-scattering model. Predicted mean equivalent spherical radius gas-bladder size varied with depth, ranging from 2.1 mm (shallow) to 0.6 mm (deep). Density of night-time organisms varied throughout the water column and were highest (0.019 m^{-3}) in the 200–300 m depth range. Predictions of 38 kHz volume-backscattering strength (Sv) from the density of gas-bladdered organisms could explain 88% of the vessel's 38 kHz Sv at this location (S 40.9, E 166.7). Catch retained by trawls highlighted the presence of gas-bladdered fish of a similar size range but different densities while optical measurements highlighted the depth distribution and biomass of gas-inclusion siphonophores. Organism behaviour and gear selectivity limits the validation of acoustic estimates. Simultaneous optical verification of multifrequency or broadband acoustic targets at depth are required to verify the species, their size and biomass.

Keywords: acoustic, fish, mesopelagic, optics, siphonophores, target strength.

Introduction

Knowledge of the structure and function of biota in the deep ocean is necessary to assist in managing human impacts, and especially to predict the behaviour of oceans in a changing climate using ecosystem models (Fulton *et al.*, 2005; Lehodey *et al.*, 2008, 2010; Maury, 2010). Development of these ecosystem models will require an understanding of the biomass of the mid-trophic groups that link primary production to top predators. Here we define the mid-trophic group as those macrozooplankton and micronekton organisms of ~2–20 cm containing cephalopods, crustaceans, and small fish but also large gelatinous organisms (Lehodey *et al.*, 2010). It is proposed that acoustic methods could help describe their biomass at a global scale, using a combination of existing or future developments (Handegard *et al.*, 2010, 2012; Lehodey and Maury, 2010; Lehodey *et al.*, 2014). An existing acoustic method uses echosounders from ships of opportunity to monitor the volume-backscattering strength at 38 kHz transiting the ocean basins (Kloster *et al.*, 2009).

Historically, the biomass of mid-trophic organisms within deep-ocean ecosystems (0–1000 m) has been estimated using

acoustics (Marshall, 1951; Andreeva, 1964; Kalish *et al.*, 1986). There has been a lot of attention on scattering layers and their diurnal vertical migrations. In particular, there has been a focus on organisms with gas-bladders that depending on frequency can make up the dominant component of the scattering (Barham, 1963; Davison *et al.*, 2015). The dominant species that cause the scattering are identified using nets, and optics as gas-bladdered fish or siphonophores with pneumatophores or a combination of both (Benoit-Bird and Au, 2001; Benfield *et al.*, 2003; Lavery *et al.*, 2007; Davison *et al.*, 2015). Each of these methods has varying selectivity, making estimates of density of the various scattering types problematic (Pakhomov and Yamamura, 2010; Kaartvedt *et al.*, 2012). Even less clear for the requirements of ecosystem characterization is the size structure and density of these gas-bladdered organisms (fish or siphonophores) and how they are organized in space and time. Current estimates of density and biomass of the gas-bladdered fish component using nets or acoustics vary by 1–2 orders of magnitude (Koslow *et al.*, 1997; Kloster *et al.*, 2009; Kaartvedt *et al.*, 2012). This difference could be due to the

different selectivity of the two gear types used. A particular problem for acoustics is resonance scattering where the scattering response is non-linear with fish size (Davison *et al.*, 2015).

Acoustic resonance volume scattering characteristics of gas bladders have been used to define the size spectra of organisms using a broadband with low- and high-frequency ranges as well as using several discrete frequencies. With these methods, it is possible to estimate the average size of the gas bladders and their equivalent spherical radius (ESR) by comparing the volume scattering frequency-response to a model (Andreeva, 1964; Holliday, 1972; Kalish *et al.*, 1986; Stanton *et al.*, 2010). Volume scattering at multiple frequencies is problematic because; sound absorption limits range propagation at higher frequencies (Francois and Garrison, 1982); the volume ensonified increases with range reducing the signal strength and increasing the number of scatterers of different species and sizes in the backscattered response. An alternative to volume scattering is to resolve single targets at multiple frequencies using split-beam systems (Demer *et al.*, 1999). Detection of single targets to depths of 1000 m requires a lowered probe to ensure only one target is within the pulse-resolution volume. Based on the number of targets at each depth, an estimate of the density of targets can be made using echo counting methods (Kloser *et al.*, 2009).

Identifying the multifrequency *in situ* targets can be done with simultaneous optical measurements. Using stereo photography, the size and orientation of the organism can be measured and related back to the target (Kloser *et al.*, 2013). These methods have worked well for large fish (>30 cm) that have been herded pass the acoustic optical system (AOS) on a net (Ryan *et al.*, 2009). What is less clear is the ability of this same system to work as a lowered probe to sample the deep-scattering layers. One issue identified was the low density of targets and the issues of avoidance to the vibration and lights without a herding net. Another issue was the more limited range resolution due to the smaller organisms to measure (2–10 cm).

In this paper, we evaluate the potential for a lowered two-frequency AOS probe to estimate the number and size of gas-bladdered organisms as a proof of concept. To do this, we compare the measured frequency-response with that of a gas-bladder resonance model, net catches, and optical sensing. Finally, these estimates of density are compared with the vessel's 38 kHz acoustics to determine the proportion of backscatter that can be attributed to different sizes of gas-bladders with depth.

Methods

Region

Detailed fine-scale acoustic and biological sampling was done as part of a programme to monitor the deep-scattering layer in the Tasman Sea. As part of this programme, a fishing vessel is providing calibrated acoustic echograms of the basin annually since 2003 (Kloser *et al.*, 2009). To assist in the interpretation of the acoustic basin-scale echograms, fine-scale measurements have been made of the biota using nets, acoustics, and optics (Kloser *et al.*, 2009; Flynn and Kloser, 2012). Measurements reported here were made at night in the eastern sector of the Tasman Sea aboard the 65 m factory freezer fishing vessel *FV Rehua* (June 2009) and the 65 m research vessel *Southern Surveyor* (July 2011) within a box bounded by 40–41°S and 161–166°E (Flynn and Kloser, 2012). The eastern sector of the Tasman Sea is in water depths >2000 m and its oceanographic context is described in detail in Flynn and Kloser (2012) with 38 kHz backscatter to 1500 m depth from the region shown in Kloser *et al.* (2009). Vessel acoustic data from both voyages in

2009 and 2011 are available on line at www.imos.org.au as the bio-acoustics component of Australia's Integrated Marine Observing System.

Vessel-mounted volume-backscattering strength

The mean volume-backscattering strength, MVBS (S_v , dB re 1 m^{-1}) just before the AOS probe experiment was obtained from 20 to 1000 m depths with a vessel-mounted Simrad 38-kHz ES60 echosounder and ES38B transducer calibrated with a standard sphere (MacLennan *et al.*, 2002). Acoustic data were collected at 2.048 ms pulse duration and transmission power of 2 kW. Data were processed in EchoView (version 4.40; Myriax, 2010) where calibration offsets were applied and absorption 9.5 dB km^{-1} and sound speed 1500 m s^{-1} used. Background noise was removed on a per-ping basis by subtracting the average S_v between 1300 and 1490 m, with time-varied gain removed (Kloser, 1996). MVBS was determined for each 20 m depth interval, i , using, n , volume-backscattering strength, S_{v_i} , values in the depth interval:

$$S_v = 10 \log_{10} \left(\frac{\sum_{j=1}^n 10^{S_{v_j}/10}}{n} \right). \quad (1)$$

AOS Probe TS and S_v measurements

In situ TS measurements of the deep-scattering layers were obtained by lowering a multifrequency AOS probe in steps to a maximum of 950 m. The AOS probe is reported in Ryan *et al.* (2009) with the results from the split beam 38 and 120 kHz transducers reported here (Figure 1, Table 1). The system was calibrated at depth with a 38.1 mm tungsten carbide sphere suspended 20 m below the transducers with target strength of -42.3 and -39.5 dB at 38 and 120 kHz, respectively. At each 100 m interval from 50 to 950 m the probe was held stationary for 5 min to ensure a large number of targets from the sphere was obtained. The non-linear changes in calibration with depth were described by a polynomial and used as a look-up table to correct the *in situ* target strength data (Ryan *et al.*, 2009). As the AOS probe was lowered to 950 m depth the 38 and 120 kHz transducers were operated at a ping rate of 9 Hz and recorded data to 50 m. *In situ* target strength data were derived using the Simrad split-beam method 2 algorithm in the Echoview acoustic-analysis software (Myriax, 2010), using settings in Table 1. Single targets from the 38 kHz and 120 kHz data were derived and recorded with depth, ping number and position relative to the centreline of the 38 kHz transducer. Targets from 38 and 120 kHz were merged when they occurred at the same range and angular position relative to the 38 kHz transducer. To minimize beam compensation errors, contamination of the calibration sphere and signal-threshold bias, only targets within 4° of the transducer axis and a range of 5–15 m were used. The TS frequency difference, ΔTS , between the TS 38 and TS 120 kHz targets was derived from the merged dataset. Given the minimum TS threshold of -75 dB at 38 kHz, only ΔTS values satisfying $\Delta TS + TS_{120 \text{ kHz}} \geq -75$ dB are possible; and similarly for the 120 kHz threshold of -85 dB. The mean S_v was calculated from the AOS probe by integrating the 38 and 120 kHz data at a range of 35–50 m as it was lowered through the water column. Values of S_v were summarized into 20 m depth bins.

Optical measurements

The stereo optical system is as described in Kloser *et al.* (2011) using two stereo Canon 400D digital SLR cameras (Figure 1). These were triggered in the 2009 experiment when the 120 kHz echosounder

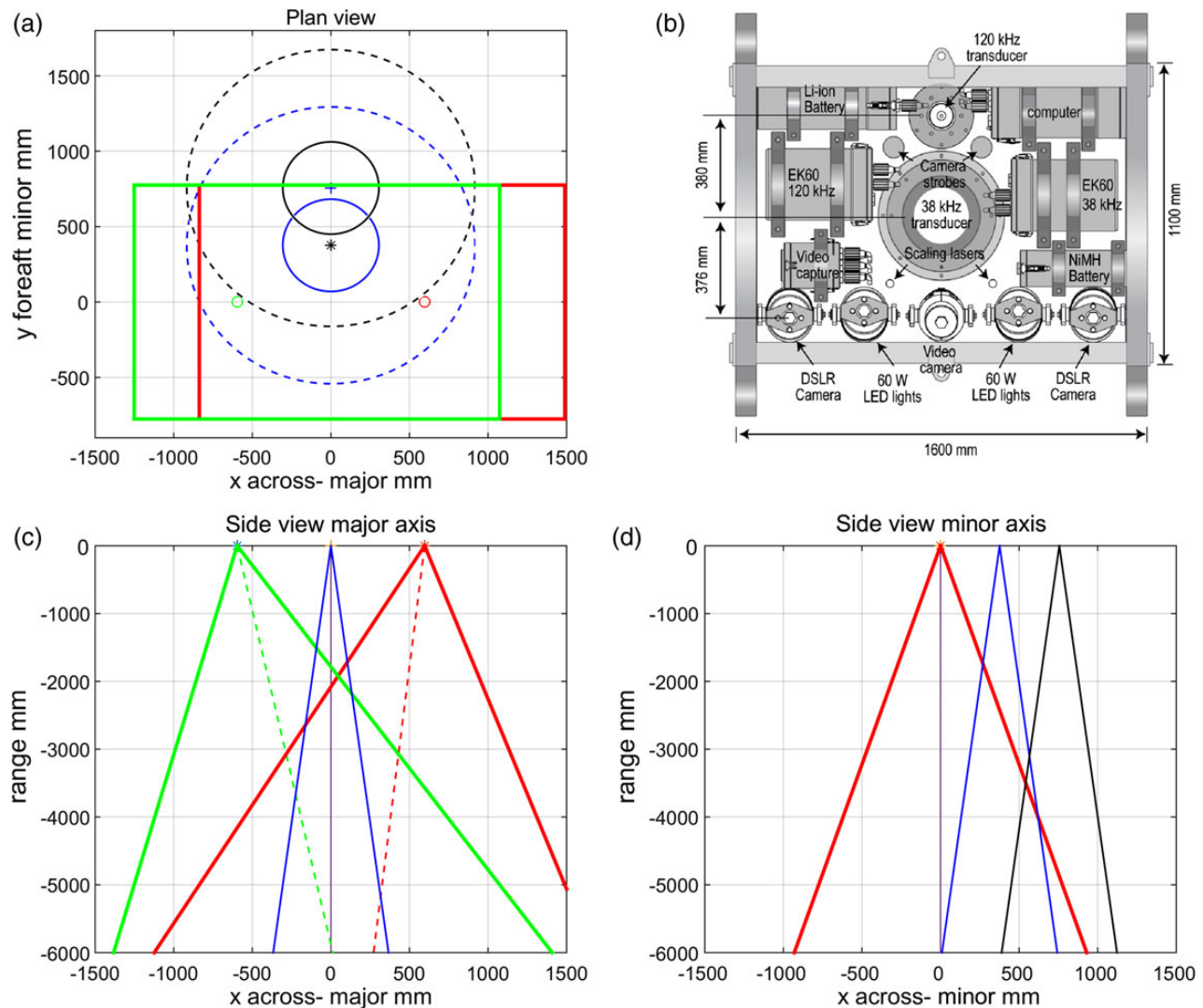


Figure 1. AOS, b, locations and separation distances of the split-beam transducers of 38 and 120 kHz and stereo cameras shown, a, sample area of the 38 kHz (asterisk, blue) and 120 kHz (cross, black) at 5 m (solid) and 15 m (dashed) and the optical sample area of the port (left green) and starboard (red right) cameras at 5 m range. (c) and (d) The acoustic and optical sampling cross-sectional area for the major (x-axis) and minor (y-axis) axis, respectively. This figure is available in black and white in print and in colour at ICES Journal of Marine Science online.

detected single-target echoes that were greater than -60 dB and between 3 and 11 m range from the transducer. The stereo-camera images allowed the use of photogrammetric methods to measure organism length and orientation. Due to technical problems with the system, only a small subset of photos were useable for stereo imagery. The system was calibrated from in-water images of a reference cube using SEAGIS CAL software and fish and siphonophore metrics taken from field images using Photomeasure software (Seager, 2008). Fish length was measured as standard length and siphonophore length was measured by the total length of the swimming bell zone. In 2011, the optical system was triggered at a 5 s interval as it was lowered through the water column to have a continuous sampling rate. Optical images were reviewed by a taxonomic expert (co-author Lisa Gershwin) to identify dominant vertebrate and invertebrate tax. Each identification was given a score between 1 (low) and 10 (high) confidence in accuracy. Here we report on the gas bearing physonect siphonophores and fish that could be identified with a confidence score >5 . An estimate of

density from the optical measures was done for the 2011 dataset where the optical detection range was 6 m and the sample-volume per image was 5.4 m^3 .

Model predictions of gas-bladder size

The following model was used to predict the resonance gas-bladder TS at 38 kHz and the logarithmic difference between 38 and 120 kHz, ΔTS , at depth z metres for ESR , a_s from 0.1 to 6 mm at 0.1 mm intervals. The target strength TS_f at frequency $f = 38$ and 120 kHz in dB form is $TS_f = 10 \log_{10}(\sigma_{bs})$ for the backscattering cross section, σ_{bs} derived from, $\sigma_{bs} = a_s^2 / [(f_{RF}/f)^2 - 1]^2 + \delta_{RF}^2 \times \text{m}^2$, at damping factor $\delta_{RF} = 0.14$. The resonance frequency, f_{RF} , was derived from $f_{RF} \approx (1/2\pi a_s)(3\gamma P_A/\rho_A)^{0.5} \text{ Hz}$, where it is assumed that the ratio of specific heat $\gamma = 1.4$, ambient pressure $P_A = 10^5(1 + 0.1z) \text{ Pa}$ at depth z , $\rho_A = 1028 \text{ kg m}^{-3}$, and a_s is the ESR of the gas-bladder volume in metres as described by Clay and Medwin (1977) (p. 221).

Table 1. Lowered AOS probe Simrad EK60 echosounder parameters, field settings, and target strength analysis criteria.

Echosounder parameter	Value		Units
Frequency	38	120	kHz
Transducer model	Simrad ES38DD	Simrad ES120-7DD	
Transducer serial number	28 332	27 386	
Pulse length	0.512	0.256	ms
Power	2000	500	W
Beam width – 3 dB	6.9/7.1 (along/athwart)	6.7/6.5	degrees
Nominal absorption	0.0099	0.0374	dB m ⁻¹
Nominal sound speed	1494	1494	m s ⁻¹
Angle sensitivity	21.9	21.0	
Single-target detection criteria	Value		Units
TS threshold	–75	–85	dB
Pulse length determination level	6	6	dB
Min. normalized pulse length	0.3	0.3	
Max. normalized pulse length	1.5	1.5	
Maximum beam compensation	12	12	dB
Maximum phase deviation minor axis	3	3	degrees
Maximum phase deviation major axis	3	3	degrees

The *ESR* of a target at depth z was assigned by matching the nearest model prediction to the *in situ* *TS* at 38 kHz and its frequency difference, ΔTS . The difference between the nearest model prediction and *in situ* measurement was retained to assess the quality of the fit. Data were summarized into 100 m depth bins from 0 to 1000 m and the density of targets and their estimated contribution to volume-backscattering strength were evaluated.

The density (d_{ij} m⁻³) of the n predicted gas bladders of radius a_{ij} (m) and target strength TS_{ij} (dB) in depth interval, i , with p_i pings is

$$d_{ij} = \frac{n}{p_i \times V} \text{m}^{-3},$$

where the overlapping insonified volume $V = 11.4 \text{ m}^3$ for the 38 and 120 kHz transducer with separation distance of 0.38 m, maximum off axis angle of 4° and target range of 5–15 m. The predicted volume-backscatter strength, Sv_i of the k predicted gas-bladder size classes for each depth interval, i , is

$$Sv_i = 10 \log 10 \left(\sum_{j=1}^k 10^{TS_{ij}/10} \times d_{ij} \right) \text{dB}. \quad (2)$$

Net sampling

Catch was retained from a pelagic trawl at night in 2009 using a commercial pelagic net with mesh sizes of 15 m at the mouth to 130 mm at the terminal end then fitted with a multiple closing codend device (MIDOC) equipped with six nets of 12 mm mesh (Flynn and Kloser, 2012). The net was deployed to 1000 m and towed to the surface with MIDOC net samples retained at each 200 m depth interval after 20 min of towing. The progress and timing of the net haul was monitored in real time with a SCANMAR acoustic-net-monitoring system. Net samples were sorted into trays of four acoustic groups: fish, crustacean, squid, and gelatinous, photographed then frozen. Thawed samples were identified to species where possible (tray photographs assisted the identification of gelatinous organisms, which were largely unidentifiable after freezing and thawing), and lengths and weights obtained. A detail species analysis of the catch is presented in Flynn and Kloser (2012) where 95% of the fish biomass of lengths <100 mm were lantern fish and 35

species had confirmed gas bladders. Species were segmented into five acoustic categories: fish with no gas bladder, fish with gas bladder, squid, crustaceans, and gelatinous. The fish component was further split into small (<10 g), medium (10 g < fish ≤ 100 g), and large (>100 g) based on weight. The density of fish with gas bladders was determined by the numbers of fish divided by the volume of water sampled, determined here as being the mouth area where the mesh size was 200 mm (~409 m²) multiplied by the distance sampled in metres. The gas-bladder volume and its *ESR* of the fish was needed to compare with those predicted by the resonance gas-bladder model. A simplified estimate of the mean gas-bladder volume of fish assumed that the bladder volume was 3% of mean fish volume (ml) assuming a density of 1.034 g ml⁻¹ for mean fish weight and the mean *ESR* derived from this volume (Davison, 2011).

Results

At night on the 18 June 2009 at 40° 57' S 166° 44' E the vessel-mounted 38 kHz mean *Sv* from 20 to 1000 m was –73.2 dB with two regions of elevated backscatter at 100–200 m and 600–800 m (Table 2 and Figure 2). In general, this agrees with the volume backscatter measured by the AOS at 38 kHz, whereas the 120 kHz is 5–10 dB lower between 300 and 900 m depth. An exception is at 350–450 m that may be due to differences in the vessel and AOS sampling volumes and patchiness of biota. The AOS probe lowered to a depth of 950 m at this site recorded 7492 targets at 38 kHz for a range of 5 m–15 m from the transducer and <4° off axis. Merging the 38 and 120 kHz target-strength datasets so that only coincident targets occurred within the overlapping beam ($\pm 4^\circ$) reduced the number of targets to 5999 which is 14% less than the number of targets expected after accounting for the 31% reduction in sampling volume of the overlapping beams.

Segmenting these targets into 100 m depth bins and converting to density shows that the distribution of 38 kHz targets changes significantly with depth (Figure 3a). Two modes of high density of targets were recorded in the 100–300 and 500–900 m depth strata's being 18 and 14.4 targets per 1000 m³, respectively (Table 3). Of note was the 5 dB increase in mean target strength of the 38 kHz data between 150 and 750 m, whereas the 120 kHz mean *TS* decreased by 3.3 dB over this depth range (Table 3).

Table 2. Summary of the mean volume reverberation (S_v dB) measured for each 100 m depth stratum using the vessel mounted sounder at 38 kHz and that measured at 35–50 m range from the AOS at 38 and 120 kHz.

Mid Depth	S_v 38 kHz dB				S_v 120 kHz dB			$S_{v_{38-120}}$ AOS
	Vessel	AOS	Pred.	AOS-pred	AOS	Pred.	AOS-pred	
50	−73.4	−76.9	−78	1.1	−80.2	−78.1	−2.1	3.3
150	−72.6	−74.4	−73.3	−1.1	−73.1	−74.6	1.5	−1.3
250	−74	−75.8	−72.4	−3.4	−76.1	−77.9	1.8	0.3
350	−76.4	−79.9	−78.1	−1.8	−83.2	−78.9	−4.3	3.3
450	−76.2	−77.4	−78.5	1.1	−80.2	−80	−0.2	2.8
550	−73.6	−70.6	−76.2	5.6	−81.4	−83.4	2	10.8
650	−70.3	−71.4	−71.4	0	−80.7	−81.4	0.7	9.3
750	−70.5	−70.8	−69.8	−1	−80.1	−80.8	0.7	9.3
850	−74.2	−73.8	−73.1	−0.7	−81	−81.8	0.8	7.2
950	−75.9	−78.3	−77	−1.3	−82.1	−88.1	6	3.8
Mean	−73.2	−73.9	−73.8		−78.6	−79.3		

The predicted S_v at 38 and 120 kHz based on the density and target strength of gas bladders is summarized in Table 3. The mean S_v of the 1000 m water column is derived for each frequency and platform. The difference between the AOS measured and model-predicted S_v and the AOS S_v frequency difference ($S_{v_{38-120}}$) is shown.

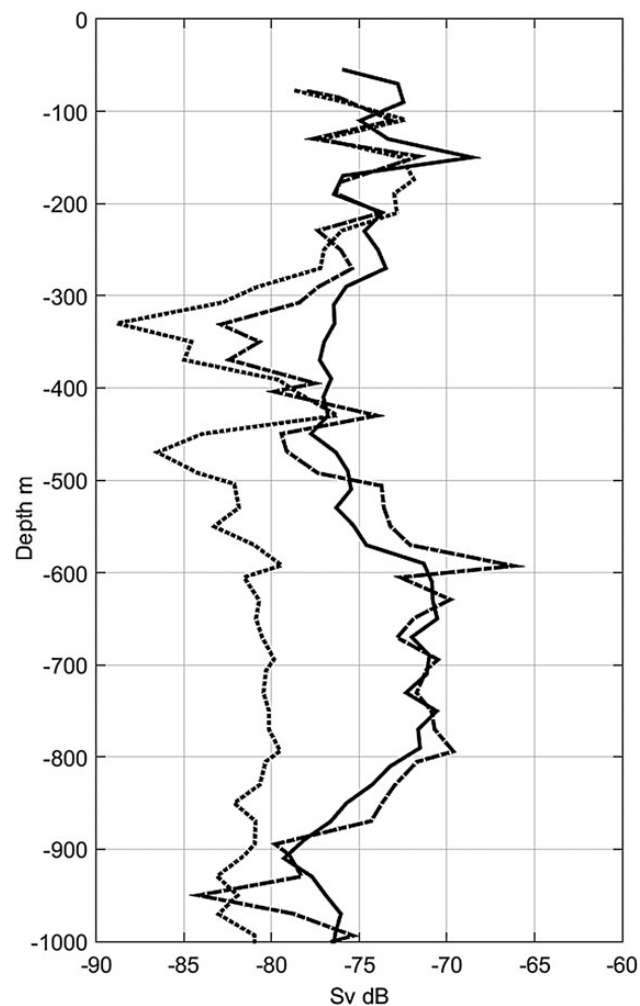


Figure 2. Mean volume backscattering strength (S_v dB re m^{-1}) in 20 m depth intervals from the 38 kHz vessel-mounted transducer just before the lowered AOS experiment (solid). Mean S_v (dB) in 20 m depth interval from the AOS (range 35–50 m) based on the 38 kHz (dot dashed) and the 120 kHz (dotted) transducers. Mean S_v of each 100 m depth intervals are given in Table 3.

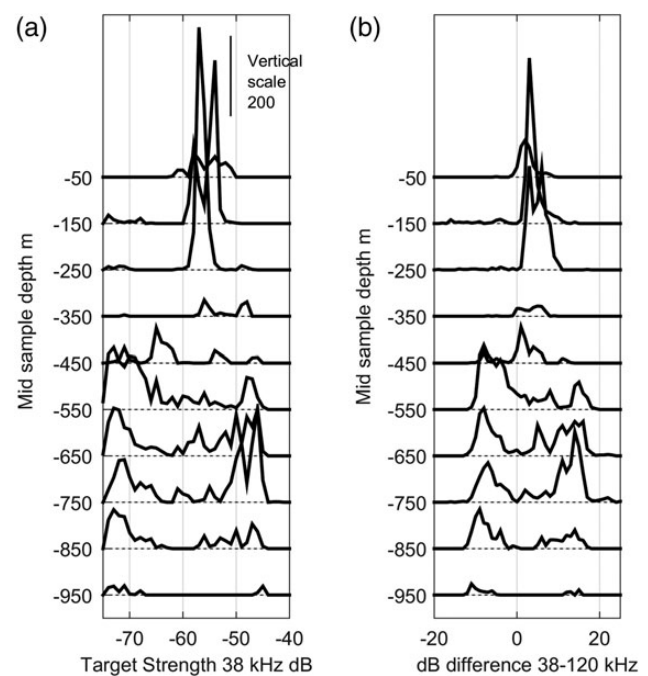


Figure 3. Number of coincident 38 and 120 kHz *in situ* targets identified at range 5–15 m from the transducer and maximum angle off axis of $4-15^\circ$ in 100 m depth bins at: (a) 38 kHz with a minimum threshold of -75 dB; (b) TS frequency difference $TS_{38} - TS_{120}$ kHz. Each 100 m bin has been offset by the mean depth. Abundance is differentiated as the height of the lines for each depth with vertical scale shown.

Hence, the TS frequency difference, ΔTS increased from 3.8 dB at 150 m depth to 11.7 dB at 750 m depth. The large difference in, ΔTS 9.0–11.8 dB for depths 500–1000 m is due to the widely spaced bimodal distribution (Figure 3b).

To interpret the field data, the model of resonance scattering was formulated to estimate the ESR of a gas bladder based on the 38 and 120 kHz frequencies. Using the model, the resonant peak of both 38 and 120 kHz increases with depth (Figure 4). At 120 kHz the frequency-resonance peak is generally 17 dB less than that of the

Table 3. Summary of the mean AOS merged *in situ* target strength (dB) and mean density for 38 and 120 kHz for each 100 m depth stratum and the model-predicted ESR (mm) and the mean model-predicted error (m_{fit}) at each depth and associated standard deviation (SD_{fit}).

Mid Depth	Targets (#)	Pings (#)	TS_{38} (dB)	TS_{120} (dB)	$TS_{38} - TS_{120}$ (dB)	Density (10^{-3} m^3)	ESR (mm)	SD (mm)	m_{fit} (dB)	SD_{fit} (dB)
50	307	5242	-54.7	-57.1	2.4	5.1	1.7	0.6	-2.1	2.2
150	958	4920	-55.4	-58.9	3.5	17.1	1.3	0.6	-1.6	2.4
250	1120	5159	-56.2	-60.8	4.6	19.0	0.8	0.5	-0.1	1.4
350	121	5127	-51.1	-53.0	1.9	2.1	2.1	1.5	-0.4	1.4
450	341	5046	-55.7	-59.4	3.7	5.9	0.8	1.1	0	1.4
550	608	4219	-54.6	-63.5	9.0	12.6	0.5	0.2	0.2	0.5
650	1053	5369	-51.7	-63.0	11.3	17.2	0.6	0.1	0.1	0.7
750	797	4645	-50.3	-62.2	11.8	15.0	0.6	0.2	-0.1	1.2
850	596	4088	-52.8	-62.5	9.7	12.8	0.6	0.2	0.1	0.4
950	98	3135	-51.4	-61.2	9.8	2.7	0.6	0.2	0.5	0.4

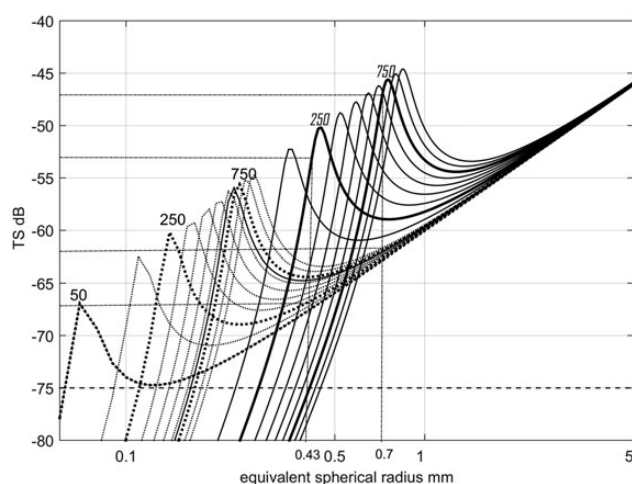


Figure 4. Predicted response of target strength for a gas bladder of ESR from 0.06 to 5 mm at depths from 50 to 950 m in 100 m increments for 120 kHz (dashed line) and 38 kHz (solid line) with depths 50, 250, and 750 m highlighted. Dashed line shows lower limit of detection threshold set for the 38 kHz transducer. Predicted ESR of the visually verified siphonophore 0.43 mm at 250 m depth (dot-dashed line) and fish 0.7 mm at 750 m depth (dot-dashed line) following measured target strength values in Table 5.

38 kHz frequency for the same depth and ESR size. As depth increases, the dB difference resonance peak shifts to larger gas-bladder sizes, changing from an ESR of 0.2 mm at 50 m depth to 0.8 mm at 1000 m depth (Figure 5). This model estimate of the relationship between target strength at 38 kHz and the TS frequency difference between 120 kHz for changing ESR gas bladders and depth helps to explain the field data (Figure 6). As depth increases the 38 kHz data fit the modelled relationship but there is a large scatter at the 100–200 m depth range. This fit to the TS frequency difference data can also be examined at 120 kHz (Figure 7). In particular, a group of scatterers in shallow waters (100–300 m depth) does not follow the observed resonance-scattering trend. These scatterers have higher target strengths at 120 kHz and may be indicative of a more fluid filled organism (e.g. small crustacean, fig. 1 of Lavery et al., 2007).

The predicted mean gas-bladder ESR for this dataset is a maximum of 2.1 mm in the 350 m depth range and a minimum of 0.5 mm at 550 m depth (Table 3). However, the distribution of predicted gas-bladder sizes are widely spaced multimodal for depths <450 m with a larger proportion of gas bladders >1 mm

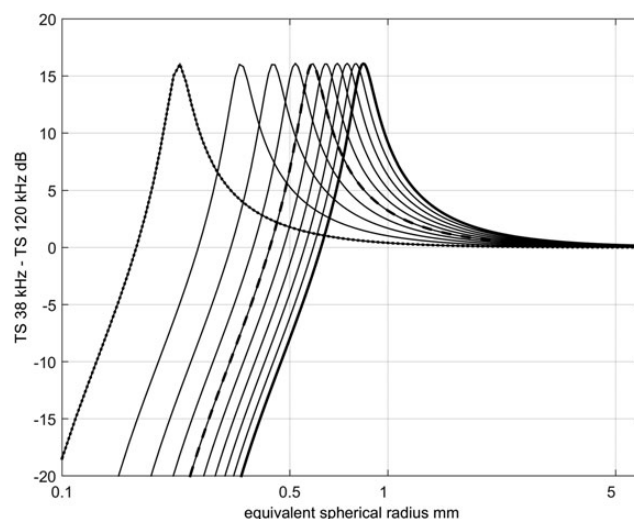


Figure 5. Predicted difference between TS at frequencies of 38 and 120 kHz for gas bladders of ESR from 0.1 to 6 mm at increasing 100 m depth intervals from 50 to 950 m (solid lines), with 450 m (dashed line) and 950 m (solid line) highlighted.

ESR with a SD of >0.5 mm (Table 5, Figure 8). At depths >450 m the spread in ESR sizes decreases which is reflected in the predicted ESR SD being small, <0.2 mm (Table 3). The detection threshold of ESR increases with depth being 0.015 mm at 50 m, increasing to 0.044 mm at 950 m (Figure 8). This change in selectivity will affect the size distribution predicted and at greater depths underestimate smaller gas bladders.

The error between model prediction and measured dB difference decreased with depth, being -1.9 dB at 50 m depth and 0.6 dB at 950 m depth (Table 3). Similarly, the standard deviation of error was high at shallow depths, 2.1 dB at 50 m, and low at greater depths, 0.5 dB at 950 m. Mismatch between model-predicted ESR and TS measurements varied within a depth range based on the ESR sizes (Figure 9). Within the 100–200 m range the ESR <0.4 mm gas-bladder size had a positive bias, whereas the ESR of 1–2 mm had a negative bias. At the 800–900 m depth range, the model fit was within 0.1 dB of the measurements with a SD of <0.4 dB (Figure 9, Table 3). Note that the minimum predicted ESR increases with depth due to the 38 kHz minimum-target threshold (Figure 9).

Based on the estimated ESR at depth and their density, the Sv at both 38 and 120 kHz was predicted using Eq. 2 (Table 2). The

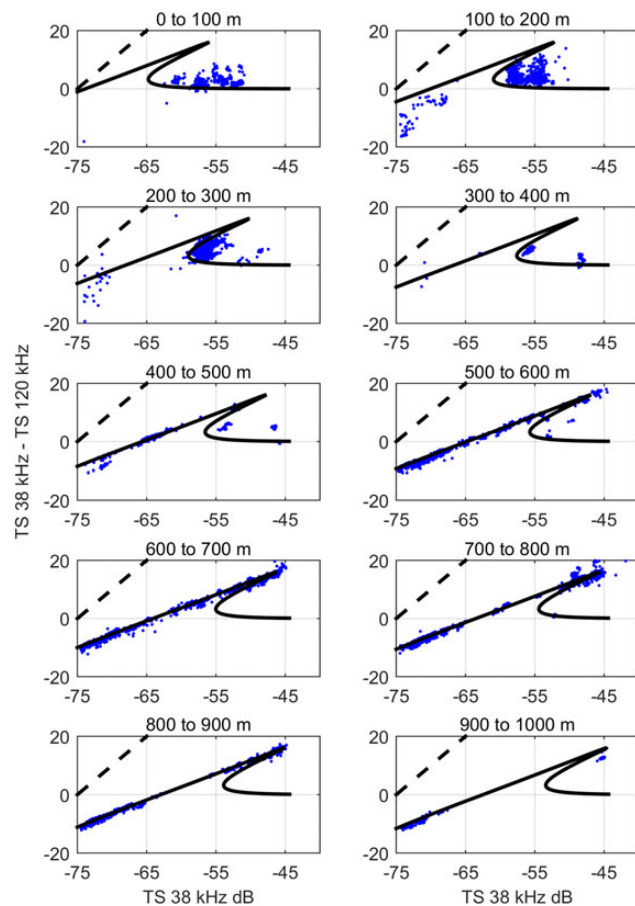


Figure 6. Scatterplot of the TS frequency difference ($TS_{38} - TS_{120}$ kHz) in 100 m depth strata to 1000 m and the predicted resonance scattering from a gas-bladder based on TS frequency difference at mid depth (solid line) as a function of *in situ* target strength data at 38 kHz. Dashed line represents the minimum detectable TS. This figure is available in black and white in print and in colour at *ICES Journal of Marine Science* online.

predicted S_v was only slightly less than that measured from the vessel-mounted transducer at 38 kHz with the mean difference over all depths being -0.5 dB or a factor of 0.88. This means that a combination of the density of targets and their target strengths represented 88% of the echo intensity measured by the vessel-mounted 38 kHz echosounder. Similarly, the predicted S_v at 38 and 120 kHz represented 98 and 86% of the measured AOS probe S_v , respectively (Table 2). The water column average 10–1000 m vessel-mounted S_v at 38 kHz was 0.7 dB higher than the AOS S_v at 38 kHz and 5.4 dB higher than the AOS S_v at 120 kHz integrated over the same depth range.

The trawl catch at the site retained a high number of small gas-bladdered fish with highest densities in the 0–200 m range of 3.3 fish per 1000 m^3 . The lowest density of small gas-bladdered fish was in the 400–600 m depth range, where there were 0.001 fish per 1000 m^3 . There is little agreement between the AOS probe densities with a range of 7.8–16.1 per 1000 m^3 and net-retained catches of 0.001–3.3 per 1000 m^3 , or the relative trend across depths (Table 4). Over a 200 m depth range, the net sample-volume was ~ 3700 times larger than the acoustic sample-volume, potentially masking any fine-scale structuring observed with the acoustics.

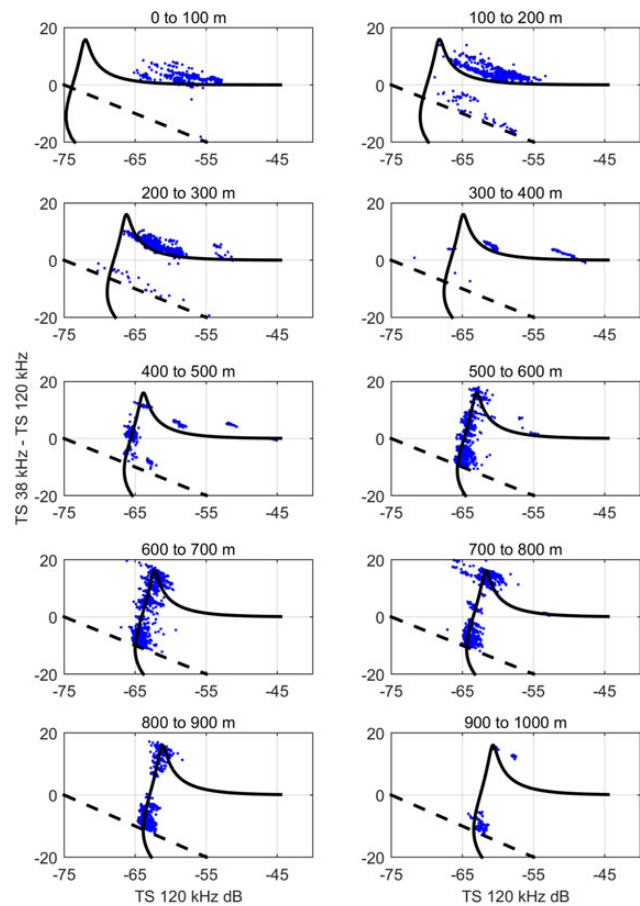


Figure 7. Scatterplot of the difference ($TS_{38} - TS_{120}$ kHz) in 100 m depth strata to 1000 m and the predicted resonance scattering from a gas-bladder based on TS frequency difference at mid depth (solid line) as a function of the *in situ* target strength data at 120 kHz. Dashed line represents the minimum TS threshold limit. This figure is available in black and white in print and in colour at *ICES Journal of Marine Science* online.

Mean gas-bladder ESR in the trawl catch ranged from 0.8 mm for small fish (0.6 g) to 3.5 mm for medium fish (47.5 g), assuming gas-bladder volume was a constant 3% of fish volume (Table 4). Estimates between resonance scattering and net-derived gas-bladder size (3% of fish volume) were similar for the small (<10 g) fish for depths <400 m, and a factor of 2 higher for depths >400 m (Tables 3 and 4). For medium fish (10 g $<$ fish < 100 g), the mean gas-bladder ESR size range of 2.5 and 3.5 mm was detected in the resonance-scattering ESR predictions at low occurrences (Figure 8).

The combined optical and acoustic measurements were confounded with technical and deployment problems in 2009 where only a small subset of optical images are available and none from the starboard camera. Within this dataset, eight images were scored as having physonect (gas bearing) siphonophore, and 11 as fish. In 2011, the camera system was operated at regular 5 s intervals between 10 and 900 m with 1086 images of which 16 were scored as having physonect siphonophores and one with fish. Siphonophore were of highest concentration in the 200–300 m depth ($n = 10$) and 600–900 m ($n = 4$) depth zones for this profile. An approximate density of the physonect siphonophores through the water

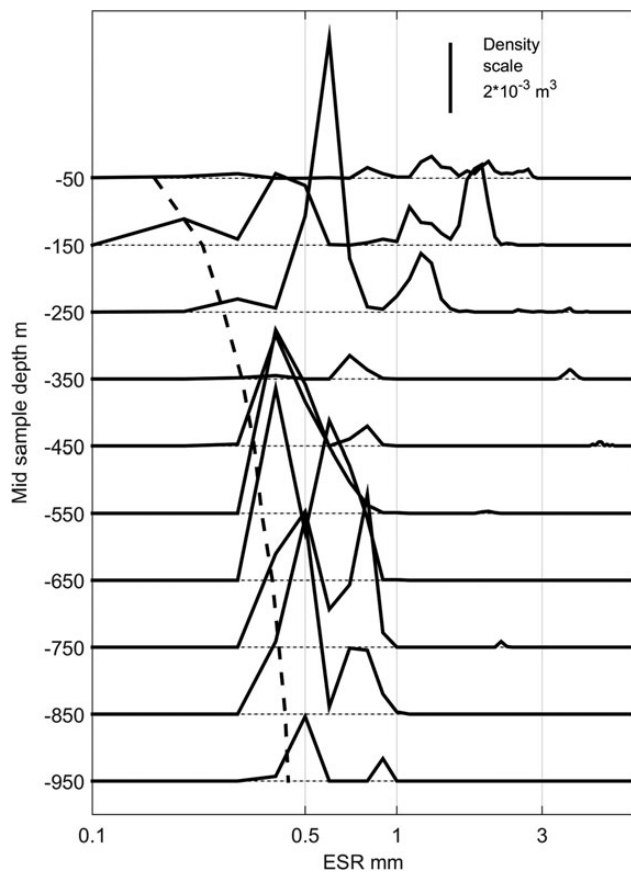


Figure 8. Density of gas-bladder sizes, as ESR (mm), based on the *in situ* TS data fitted to the model in 100 m depth ranges to 1000 m (solid lines). The threshold of minimum ESR detection capability at mid sample depth at 38 kHz shown as dashed line.

column is 2.5 per 1000 m³ for an average water-column depth of 10–900 m.

The resonance scattering of a visually verified siphonophore and fish (Figure 10) with target strengths at two frequencies were sourced from the datasets and summarized in Table 5. Based on the target strength at 38 and 120 kHz and their difference, the gas-bladder ESR can be estimated from the resonance-scattering model (Table 5, Figure 4). For these two examples, the estimated gas-bladder ESR for the fish at 750 m is 0.7 mm and for the siphonophore at 257 m is 0.43 mm. If the mean siphonophore target strength is –52.7 dB at 38 kHz and the density is 2.5 per 1000 m³, the expected mean water-column volume backscatter is expected to be –78.7 dB.

Discussion

Using a two-frequency AOS probe, it is possible for the 2009 dataset to associate 88% of the volume scattering at 38 kHz to small gas bladders of mean ESR from 0.5 to 2.1 mm. These gas bladders may be associated with a combination of fish and gelatinous zooplankton. Net catches were dominated by gas-bladdered fish with mean body weight of 0.6–48 g and an estimated mean ESR of 0.8–3.5 mm. There was a large discrepancy in the estimate of the density of gas-bladdered targets; the range was 7.8–16.1 per 1000 m³ for the AOS probe and 0.001 to 3.3 per 1000 m³ for the nets. These differences could be due to both methodological and

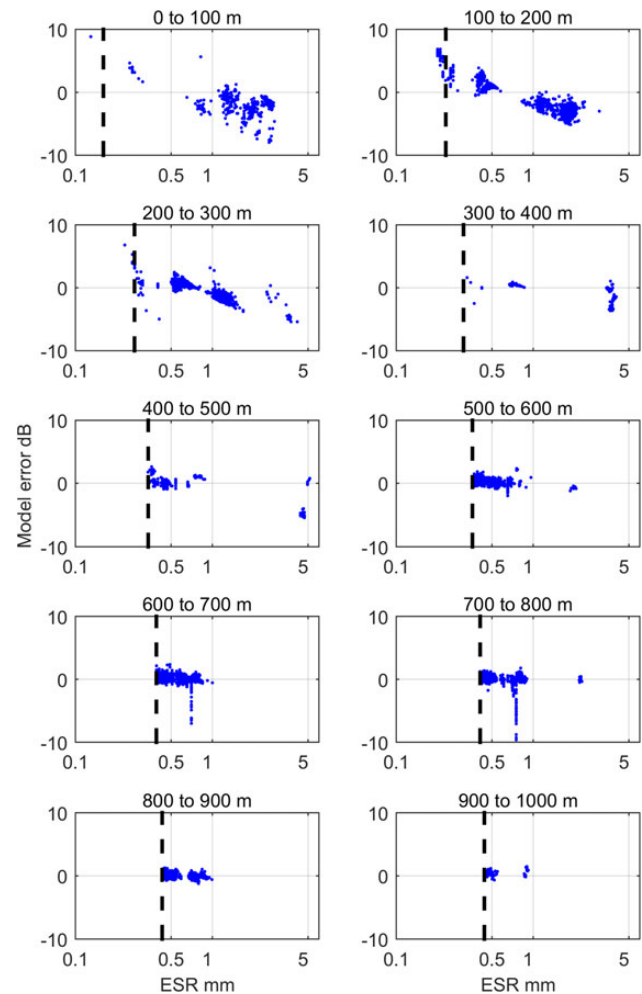


Figure 9. Scatterplot of the fit of the *in situ* TS frequency difference data to the model-predicted ESR (mm) in 100 m depth ranges to 1000 m. The limit of detection for 38 kHz is shown as a dashed line. This figure is available in black and white in print and in colour at ICES Journal of Marine Science online.

sampling biases from both the net and acoustic sampling devices. The optical system in 2011 recorded a density of physonect siphonophores of 2.5 per 1000 m³ from 10–900 m depth. All these ESR size range and density measurements will have selectivity and catchability biases that need further quantification.

Our prediction of the gas-bladder ESR size using the resonance-scattering model and *in situ* target strengths at two frequencies is consistent with the findings of other studies that have used broadband and target phase measurements (Kalish *et al.*, 1986; Barr and Coombs, 2005). The advantage of the lowered AOS probe approach used here is the ability to identify individual targets, infer their gas-bladder size, and measure their numeric density. Perhaps the exact size of the gas bladders will deviate due to incomplete knowledge of the resonance properties of the gas bladder and surrounding tissue. It is also possible that small and large non-gas-bladdered organisms could be inferred as having a gas bladder when they do not. Hence, a further exploration of this work would be to look at the deviation from a suit of models at each depth range and to determine if a further refinement could be done in predicting these properties including the organisms' body. Ideally, more frequencies with

Table 4. Summary of the numbers and mean weight (g) retained in the trawl catch for the dominant medium (M) and small (S) gas-bladdered species for each 200 m depth stratum from 1000 m depth to the surface.

Sample range		Catch								AOS Density (10 ⁻³ m ³)
Depth (m)		Numbers		Mean weight		Estimated ESR (mm)		Density (10 ⁻³ m ³)		
Start	End	M	S	M	S	M	S	M	S	
200	0	5	4372	45.0	0.6	3.5	0.8	0.004	3.300	11.1
400	200	10	182	13.0	4.3	2.3	1.6	0.010	0.182	10.6
600	400	4	1	15.0	5.0	2.4	1.7	0.004	0.001	9.3
800	600	2	19	47.5	3.2	3.5	1.4	0.002	0.019	16.1
1000	800	9	32	20.6	1.7	2.7	1.2	0.012	0.041	7.8

Estimates of the ESR (mm) of the gas-bladder assuming gas-bladder volume was 3% of the fish volume. Estimated trawl catch density (per 1000 m^3) of gas-bladdered fish and AOS probe density (Table 2) were derived.

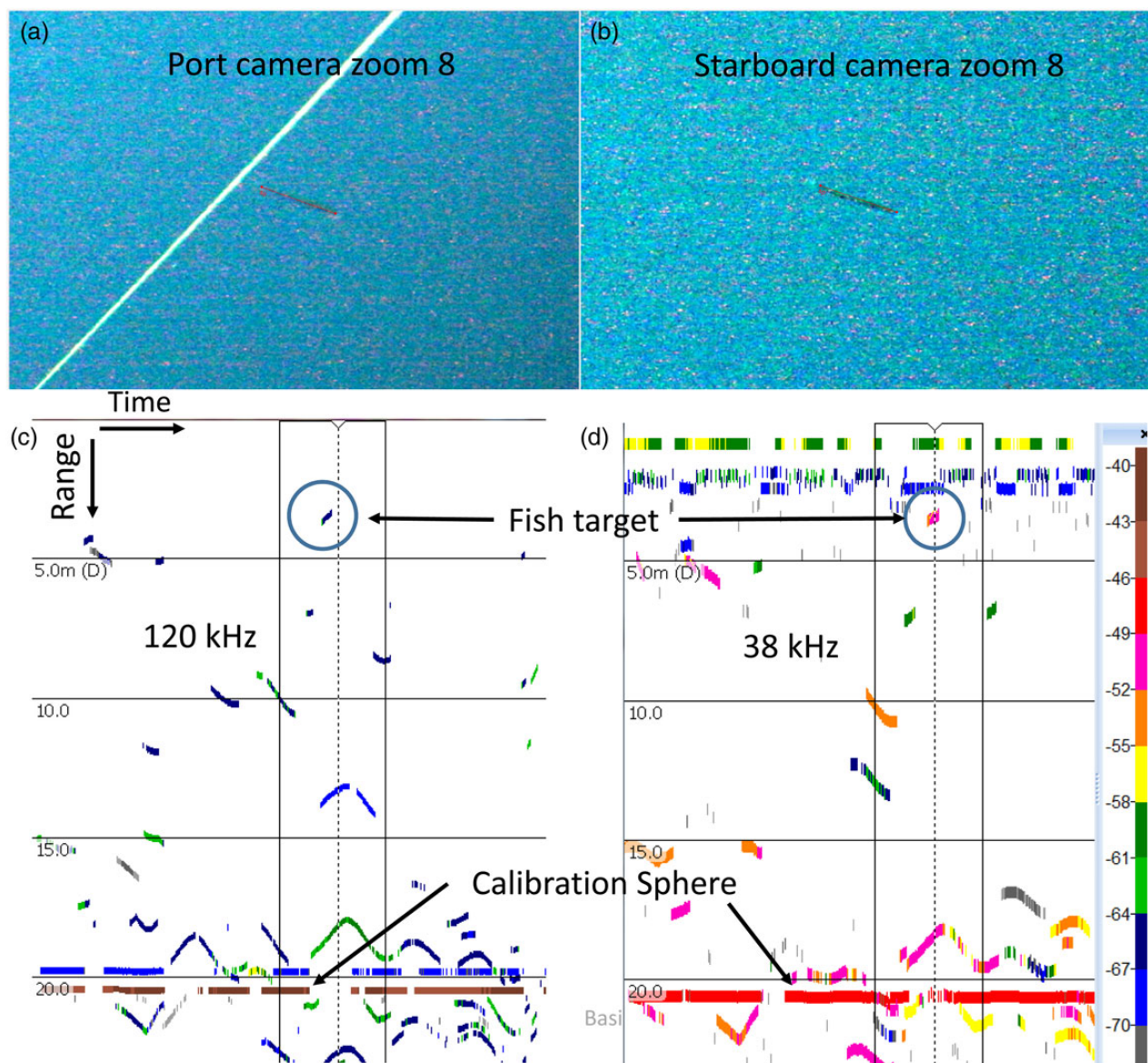


Figure 10. Example of the visually verified target strength of a fish at 750 m depth and 3 m range from the transducer with the, a, port camera image and, b, starboard camera image with eight times zoom. The acoustic echograms at, c, 120 kHz and, d, 38 kHz highlighting the fish target in a circle and the calibration sphere at range 21 m.

Table 5. Visually verified target strength at 38 and 120 kHz for a fish and physonect siphonophore with a predicted gas-bladder size based on Figure 4.

Taxa	Depth (m)	Range (m)	Length (mm)	TS 38 (dB)	TS 120 (dB)	TS 38 — TS 120 (dB)	Predicted ESR (mm)
Physonect siphonophore	257	6	73	−52.7	−66.8	14.1	0.43
Fish	750	3	35	−46.8	−61.6	14.8	0.7

Fish length is measured as standard length and physonect siphonophore length is measured as body length of the swimming bells.

broader bandwidths would be used as well as visual verification of the targets at depth with stereo cameras (Kloser *et al.*, 2011). In this way, orientation of the targets and effects of prolate spheroid gas bladders could be investigated, based on the morphology of fish or siphonophore gas bladders.

Our use of only two frequencies to make model estimates is problematic due to signal-to-noise thresholding effects. The minimum ESR size that could be predicted ranged from 0.2 mm at 150 m depth to 0.45 mm at 950 m depth. This represents a selectivity bias in the method, and more frequencies are required to cover the smaller size-range at depth. In this case, it appears from the data that a mode of gas-bladder sizes in the 0.4 mm ESR size range is gradually reduced with depth due to a thresholding bias of the 38 kHz transducer. An additional, higher frequency would be needed to alleviate this.

Sampling biases, differing between net catches and acoustics sampling, have been well reported for macrozooplankton and micronekton (Pakhomov and Yamamura, 2010; Kaartvedt *et al.*, 2012). Therefore, we cannot be certain that the trawl will retain all the macrozooplankton and micronekton in the water column, nor if the proportions are representative. Hence, comparison of net catches and acoustics is problematic for these diverse, mixed-species mesopelagic communities of macrozooplankton and micronekton. This would be a problem in this case due to the 10 mm codend meshes for small fish and larvae fish. In particular for the small and translucent bristlemouth (*Cyclothone* sp.) retained in the trawl that has a gas bladder and been reported as the cause of resonance scattering at depth (Peña *et al.*, 2014). For the gelatinous community, it is often difficult to recognize species due to extrusion or damage from the catch. Hence, it is difficult to know how many siphonophores with pneumatophores may be in the water column. Our optical sampling showed that gas bearing siphonophores occur throughout the water column in this region and could be responsible for a significant portion of the backscattering at 38 kHz due to resonance scattering. Siphonophores have been reported to have gas-bladder ESR ranging in ESR from 0.05 to 1.4 mm (Clay and Medwin, 1977; Benfield *et al.*, 2003; Lavery *et al.*, 2007). This overlaps with the predictions of gas-bladder sizes observed from our measurements and the visually verified siphonophore at 257 m of ESR 0.43 mm. Mesopelagic micronektonic fish can also have a varied gas-bladder ESR size range that has been reported between 0.2 and 6 mm and, from net catches, these are known to contribute to the resonance scattering observed (Kalish *et al.*, 1986; Barr and Coombs, 2005). The size range of biota detected with the optics used needs further investigation as only large siphonophores ($\sim > 50$ mm body swim bell length) were observed in this study. Avoidance of biota to the AOS probe is also an area that needs further investigation.

A major issue with attribution to gas-bladdered organisms is determining the size of the bladder depending on the depth, and whether organisms migrate with their gas bladders maintained at a constant mass, volume, or mixture of the two (Clay and Medwin, 1977). The resonance-scattering characteristics will change with

frequency, depth, surrounding tissue, gas in the bladder and bladder eccentricity. It may be possible to resolve gas-bladder resonance from different types of scatterers with the same gas-bladder volume, such as fish and zooplankton, based on the frequency characteristics. Detailed *in situ* optical verification of the targets at depth is needed to build-up a library of organisms and spectral signatures, by depth and time of day to resolve this problem. Our overly simplistic assumption in this example, where we assume 3% of fish' body volume determines the gas-bladder volume, could be improved. Although the uncertainties in the assumptions of neutral buoyancy in estimates of gas-bladder volume limits the utility of these measurements and would be best done in conjunction with optical verified target-strength measurements at depth (Kloser *et al.*, 2011).

Despite the issues raised above, this method of estimating the number of gas bladder and their size should improve our knowledge of the composition of mesopelagic micronekton communities. In this case, we have attributed 88% of the volume-backscattering strength at 38 kHz to gas-bladdered organisms. From the trawl catch, some of these gas-bladdered targets can be attributed to small and medium size fish and from optics to siphonophores. It is noteworthy that the optics imaged few fish presumably due to avoidance or lower densities. An obvious next step is to continue to verify the acoustic targets with optical sensors as well as having independent optical estimates of density for gelatinous taxa. This has been challenging for the small targets, as the range used for acoustic detection was 5–15 m poorly overlaps the optical range of typically < 6 m (Figure 1). The AOS instrument used was designed for fisheries target strength and biomass estimation and had a 7° beam opening. Wider beam opening transducers would provide more sampling overlap between the optics and acoustics. The deployment of the system with a fixed cable to the ship was also problematic due to the drift and heave of the vessel. An autonomous profiling float would be another next step in the development of this method.

The water-column profiles demonstrate the effect of resonance scattering on the 38 kHz data and how it over represents the density of organisms as a proportion of volume-backscattering strength at depth compared with the 120 kHz data. The conversion of 38 kHz volume-backscattering strength into biological units will not be linear across this depth range (Davison *et al.*, 2015). At higher frequencies, it is suggested that the volume-backscattering strength can be directly converted to biological units, but at lower frequencies this is problematic due to resonance scattering (Benoit-Bird and Au, 2002). Interpretation of the vessel-mounted 38 kHz backscatter for biological units over this large range of depths will require further investigation before robust estimates can be made (Handegard *et al.*, 2012; Davison *et al.*, 2015).

Simple attribution of the vessel-mounted 38 kHz backscatter to all fish is not supported in this work as has been done previously in this region (Kloser *et al.*, 2009; Irigoien *et al.*, 2014). Estimates of mesopelagic fish biomass based on vessel-mounted 38 kHz volume backscatter vary greatly in the Tasman Sea region from $\sim 200 \text{ g m}^{-2}$, Irigoien *et al.* (2014) and $16\text{--}19 \text{ g m}^{-2}$, Kloser *et al.* (2009). In this work, assuming all the vessels 38 kHz volume

backscatter are from fish, with a gas bladder 3% of fish volume, yields a biomass of $\sim 3 \text{ g m}^{-2}$. Resolution of this 2 order of magnitude difference in biomass estimates is needed before using these estimates in ecosystem models or for estimates of trophic efficiency.

Conclusion

A two-frequency AOS probe was used to estimate the size and number of gas-bladdered organisms in the open ocean. In this example, 88% of the vessel-mounted 38 kHz volume-backscattering strength could be attributed to gas bladders of 0.5–2.1 mm ESR. Attribution of these gas-bladder size-estimates to species is problematic due to limitations in net and optical sampling. The non-linear relationship with depth between organism density and the 38 kHz signal strength limits the prediction of biological units. Simultaneous optical verification of *in situ* targets would advance interpretation of the biological units associated with acoustic scattering in the open ocean.

Acknowledgements

This work was supported by the CSIRO's Oceans and Atmosphere Flagship and in particular we thank Dr D. Smith and initial reviews from Dr A. Butler and Dr P. Craig. The Science Equipment and Technology team of Matt Sherlock and Jeff Cordell ensured that the AOS probe could operate on fishing vessels. Mark Lewis and Caroline Sutton are thanked for collecting and recording the biological samples. The fishing vessel time was arranged through Les Scott and Graham Patchell from Petuna Longline and Sealord NZ, respectively. The RV Southern Surveyor time was provided by the CSIRO's Marine National Facility. This work contributes to Australia's Integrated Marine Observing System (IMOS) and in particular the ship of opportunity bio-acoustic programme.

References

- Andreeva, I. B. 1964. Scattering of sound by air bladders of fish in deep sound-scattering ocean layers. *Soviet Physics-Acoustics*, 10: 17–20.
- Barham, E. G. 1963. Siphonophores and deep-scattering layer. *Science*, 140: 826–828.
- Barr, R., and Coombs, R. F. 2005. Target phase: an extra dimension for fish and plankton target identification. *Journal of the Acoustical Society of America*, 118: 1358–1371.
- Benfield, M. C., Lavery, A. C., Wiebe, P. H., Greene, C. H., Stanton, T. K., and Copley, N. J. 2003. Distributions of physonect siphonulae in the Gulf of Maine and their potential as important sources of acoustic scattering. *Canadian Journal of Fisheries and Aquatic Sciences*, 60: 759–772.
- Benoit-Bird, K. J., and Au, W. W. L. 2001. Target strength measurements of Hawaiian mesopelagic boundary community animals. *Journal of the Acoustical Society of America*, 110: 812–819.
- Benoit-Bird, K. J., and Au, W. W. L. 2002. Energy: converting from acoustic to biological resource units. *Journal of the Acoustical Society of America*, 111: 2070–2075.
- Clay, C. S., and Medwin, H. 1977. *Acoustical Oceanography*. John Wiley and Sons, New York, USA. 544 pp.
- Davison, P. 2011. The specific gravity of mesopelagic fish from the northeastern Pacific Ocean and its implications for acoustic backscatter. *ICES Journal of Marine Science*, 68: 2064–2074.
- Davison, P., Koslow, T. A., and Kloser, R. J. 2015. Acoustic biomass estimation of mesopelagic fishes: backscattering from individuals populations, and communities. *ICES Journal of Marine Science*, 72: 1413–1424.
- Demer, D., Soule, M., and Hewitt, R. 1999. A multiple-frequency method for potentially improving the accuracy and precision of *in situ* target strength measurements. *The Journal of the Acoustical Society of America*, 105: 2359.
- Flynn, A. J., and Kloser, R. J. 2012. Cross-basin heterogeneity in lanternfish (family Myctophidae) assemblages and isotopic niches ($\delta^{13}\text{C}$ -13 and $\delta^{15}\text{N}$ -15) in the southern Tasman Sea abyssal basin. *Deep-Sea Research Part I-Oceanographic Research Papers*, 69: 113–127.
- Francois, R. E., and Garrison, G. R. 1982. Sound absorption based on ocean measurements. Part II: boric acid contribution and equation for total absorption. *The Journal of the Acoustical Society of America*, 72: 1879–1890.
- Fulton, E., Smith, A., and Punt, A. 2005. Which ecological indicators can robustly detect effects of fishing. *ICES Journal of Marine Science*, 62: 540–551.
- Handegard, N. O., Buisson, L. D., Brehmer, P., Chalmers, S. J., De Robertis, A., Huse, G., Kloser, R., *et al.* 2012. Towards an acoustic-based coupled observation and modelling system for monitoring and predicting ecosystem dynamics of the open ocean. *Fish and Fisheries*, 14: 605–615.
- Handegard, N. O., Demer, D. A., Kloser, R. J., Lehodey, P., Maury, O., and Simard, Y. 2010. Toward a global ocean ecosystem mid-trophic automatic acoustic sampler (MAAS). Ed. by J. Hall, D. E. Harrison, and D. Stammer. ESA Publication, Venice. In *Proceedings of OceanObs'09: Sustained Ocean Observations and Information for Society*, 2.
- Holliday, D. V. 1972. Resonance structure in echoes from schooling pelagic fish. *Journal of the Acoustical Society of America*, 51: 1322.
- Irgoien, X., Klevjer, T. A., Rostad, A., Martinez, U., Boyra, G., Acuna, J. L., Bode, A., *et al.* 2014. Large mesopelagic fishes biomass and trophic efficiency in the open ocean. *Nature Communications*, 5: 3271.
- Kaartvedt, S., Staby, A., and Aksnes, D. L. 2012. Efficient trawl avoidance by mesopelagic fishes causes large underestimation of their biomass. *Marine Ecology Progress Series*, 456: 1–6.
- Kalish, J. M., Greenlaw, C. F., Percy, W. G., and Vanholliday, D. 1986. The biological and acoustical structure of sound scattering layers off Oregon. *Deep-Sea Research Part A-Oceanographic Research Papers*, 33: 631–653.
- Kloser, R. J. 1996. Improved precision of acoustic surveys of benthopelagic fish by means of a deep-towed transducer. *ICES Journal of Marine Science*, 53: 407–413.
- Kloser, R. J., Macaulay, G. J., Ryan, T. E., and Lewis, M. 2013. Identification and target strength of orange roughy (*Hoplostethus atlanticus*) measured *in situ*. *The Journal of the Acoustical Society of America*, 134: 97–108.
- Kloser, R. J., Ryan, T. E., Macaulay, G. J., and Lewis, M. E. 2011. *In situ* measurements of target strength with optical and model verification: a case study for blue grenadier, *Macruronus novaezelandiae*. *ICES Journal of Marine Science*, 68: 1986–1995.
- Kloser, R. J., Ryan, T. E., Young, J. W., and Lewis, M. E. 2009. Acoustic observations of micronekton fish on the scale of an ocean basin: potential and challenges. *ICES Journal of Marine Science*, 66: 998–1006.
- Koslow, J. A., Kloser, R. J., and Williams, A. 1997. Pelagic biomass and community structure over the mid-continental slope off southeastern Australia based upon acoustic and midwater trawl sampling. *Marine Ecology-Progress Series*, 146: 21–35.
- Lavery, A. C., Wiebe, P. H., Stanton, T. K., Lawson, G. L., Benfield, M. C., and Copley, N. 2007. Determining dominant scatterers of sound in mixed zooplankton populations. *Journal of the Acoustical Society of America*, 122: 3304–3326.
- Lehodey, P., Conchon, A., Sennia, I., Domokos, R., Calmettes, B., Jouanno, J., Hernandez, O., *et al.* 2014. Optimization and evaluation of a micronekton model with acoustic data. *ICES Journal of Marine Science*, 72: 1399–1412.
- Lehodey, P., and Maury, O. 2010. Climate impacts on oceanic top predators (CLIOTOP): introduction to the special issue of the CLIOTOP

- International Symposium, La Paz, Mexico, 3–7 December 2007 Preface. *Progress in Oceanography*, 86: 1–7.
- Lehodey, P., Murtugudde, R., and Senina, I. 2010. Bridging the gap from ocean models to population dynamics of large marine predators: a model of mid-trophic functional groups. *Progress in Oceanography*, 84: 69–84.
- Lehodey, P., Senina, I., and Murtugudde, R. 2008. A spatial ecosystem and populations dynamics model (SEAPODYM) – modeling of tuna and tuna-like populations. *Progress in Oceanography*, 78: 304–318.
- MacLennan, D. N., Fernandes, P. G., and Dalen, J. 2002. A consistent approach to definitions and symbols in fisheries acoustics. *ICES Journal of Marine Science*, 59: 365.
- Marshall, N. B. 1951. Bathypelagic fishes as sound scatterers in the ocean. *Journal of Marine Research*, 10: 1–17.
- Maury, O. 2010. An overview of APECOSM, a spatialized mass balanced “Apex Predators ECOSystem Model” to study physiologically structured tuna population dynamics in their ecosystem. *Progress in Oceanography*, 84: 113–117.
- Myriax. 2010. Echoview 4.90 Acoustic Processing Software. Myriax Pty Ltd. GPO Box 1387 Hobart, Tasmania, Australia, 7001.
- Pakhomov, E., and Yamamura, O. 2010. Report to the advisory panel on micronekton sampling inter-calibration experiment. PICES Scientific report No. 38 North Pacific Marine Science Organisation (PICES), Sidney, BC.
- Peña, M., Olivar, M. P., Balbín, R., López-Jurado, J. L., Iglesias, M., Miquel, J., and Jech, J. M. 2014. Acoustic detection of mesopelagic fishes in scattering layers of the Balearic Sea (western Mediterranean). *Canadian Journal of Fisheries and Aquatic Sciences*, 71: 1–12.
- Ryan, T. E., Kloser, R. J., and Macaulay, G. J. 2009. Measurement and visual verification of fish target strength using an acoustic-optical system attached to a trawl net. *ICES Journal of Marine Science*, 66: 1238–1244.
- Seager, J. W. 2008. SEAGIS CAL and Photomeasure stereo photogrammetric calibration and analysis software. SEAGIS Pty Ltd. www.seagis.com.au.
- Stanton, T. K., Chu, D., Jech, J. M., and Irish, J. D. 2010. New broadband methods for resonance classification and high-resolution imagery of fish with swimbladders using a modified commercial broadband echosounder. *ICES Journal of Marine Science*, 67: 365–378.

Handling editor: David Demer